AIMS Biophysics

AIMS Biophysics, 12(1): 1–13.
DOI: 10.3934/biophy.2025001
Received: 14 October 2024
Revised: 01 December 2024
Accepted: 12 December 2024
Published: 18 December 2024

http://www.aimspress.com/journal/biophysics

Research article

Effect of changing the alternating electric current frequency on the viability of human liver cancer cell line (HEPG2)

Moataz M. Fahmy[1], Sohier M. El-Kholey[1], Seham Elabd[2,*] and Mamdouh M. Shawki[1,*]

[1] Medical Biophysics Department, Medical Research Institute, Alexandria University, Alexandria City, Egypt
[2] Physiology Department, Medical Research Institute, Alexandria University, Alexandria City, Egypt

* **Correspondence:** Email: mamdouh971@hotmail.com, seham.elabd@alex-mri.edu.eg; Tel: +00201123034145, +00201229861303.

Abstract: Different effects of alternating electric currents (AC) on biological materials have been observed depending on the frequency used. Extremely low frequencies (less than 1 KHz) produce electro-endocytosis at 500 Hz because of membrane depolarization. Intermediate frequencies coincide with tiny particle alignments and cell rotations (also known as the pearl chain effect), thus leading to the tumor-treating fields at 100–300 KHz. High frequencies (i.e., above several MHz) cause tissue heating to predominate due to the dielectric losses. This study investigates how exposure to a wide range of AC electric field frequencies affects the permeability and viability of hepatocellular carcinoma HEPG2 cells. With two silver/silver chloride electrodes, the cells were exposed to a square pulse with a magnitude of 0.4 V/cm at various frequencies between 1 Hz and 1 MHz. A dielectric properties measurement, flow cytometry analysis, fluorescent microscopy, and a polymerase chain reaction (PCR) gene expression analysis were performed. The results showed that all the exposed groups experienced a great reduction in the normal cells, with a clear increase in necrosis and apoptosis compared to the control group. It was noticed that the anti-tumoral effect of the examined frequency range was maximum at 10 KHz and 100 KHz. The permeability was increased in the groups exposed to frequencies above 1 kHz. The viability and permeability results were correlated to the electric relative permittivity, electric conductivity, and gene expression of cyclins A, B, and E.

Keywords: electric field frequency; hepatocellular carcinoma HEPG2; dielectric properties; cell viability; cell permeability

1. Introduction

Liver cancer ranks sixth in terms of the frequency of diagnosis and is the fourth leading cause of cancer-related deaths worldwide. Liver cancer is expected to affect more than a million individuals annually by 2025 [1]. Around the world, hepatocellular carcinoma (HCC), which makes up 75–85% of all primary liver cancers, is a serious public health issue [2]. The five-year survival rate of patients with HCC has not improved, even with the availability of several therapeutic options over the past twenty years, including chemotherapy, microwave ablation, and tumor removal [3]. Therefore, finding novel targets for HCC therapy is essential to reduce the disease's high rate of metastasis and recurrence.

Throughout the past 20 years, research on the biological consequences of low- and middle-frequency ranges has altered our knowledge of how to apply electric field frequencies, including 500 Hz electroendocytosis and 100–300 KHz tumor-treating fields techniques. The low-frequency 500 Hz electric field can induce reversible alterations in the plasma membrane to allow for the direct passage of the molecules of interest into the cell cytosol [4]. The moderate-frequency 100–300 KHz effectively inhibited the growth of cancer cells both in vitro (using cell cultures obtained from melanoma, glioma, lung, prostate, and breast cancer) and in vivo [5].

In the resistor-capacitor (RC) model of the biological cells, the cell membrane acts as a capacitor that varies according to the expression of lipid bilayers and membrane proteins, while the cytoplasm functions as a resistor, thereby reflecting the expressions of cytoskeleton proteins, nuclear components, and ionic concentrations inside cytoplasm membranes [6]. Therefore, possible changes in the components of cancer cells can be expected with specific signature changes that are believed to affect their electrical properties. One of the earliest observations of such changes was the reduced transmembrane potential of cancer cells, which correlates well with their high mitotic activity [7].

The application of an external electric field can lead to changes in the dielectric properties of cancerous cells, which is a major part of the electric properties of the cells; this is dependent on cell membranes (α- and β-dispersions) and cell composition (e.g., water, ions). In turn, these electrical changes can cause physiological changes [8]. The impact of the applied electric field is a frequency-dependent.

For a better understanding of the electric field action on tumor cells, a wide range of frequencies should be applied to detect the gradual impact or the most effective frequency on the cells' permeability and viability. In this work, our goal is to identify the potential biophysical and genetic mechanisms of action while examining the impact of a broad range of alternating electric field frequencies (1 Hz–1 MHz) on the viability and permeability of an HCC cell line (HEPG2).

2. Materials and methods

2.1. Electric exposure system

Electric fields with different conditions were delivered through a pair of plate silver/silver chloride electrodes with a 1.5 cm^2 surface area. The distance between the two electrodes was 5 cm. Two holes in the lid of the cell culture dish were made, and the two electrodes were passed through them and then fixed. Each electrode was connected to one output terminal of the digital function generator (CALTEK, CA1640P-02 function generator/counter, serial number: 06mg0676, USA). The applied electric field was bipolar square waves of 0.4 V/cm for 5 minutes. The frequency of exposure ranged from 1 Hz to 1 MHz, as shown in Figure 1.

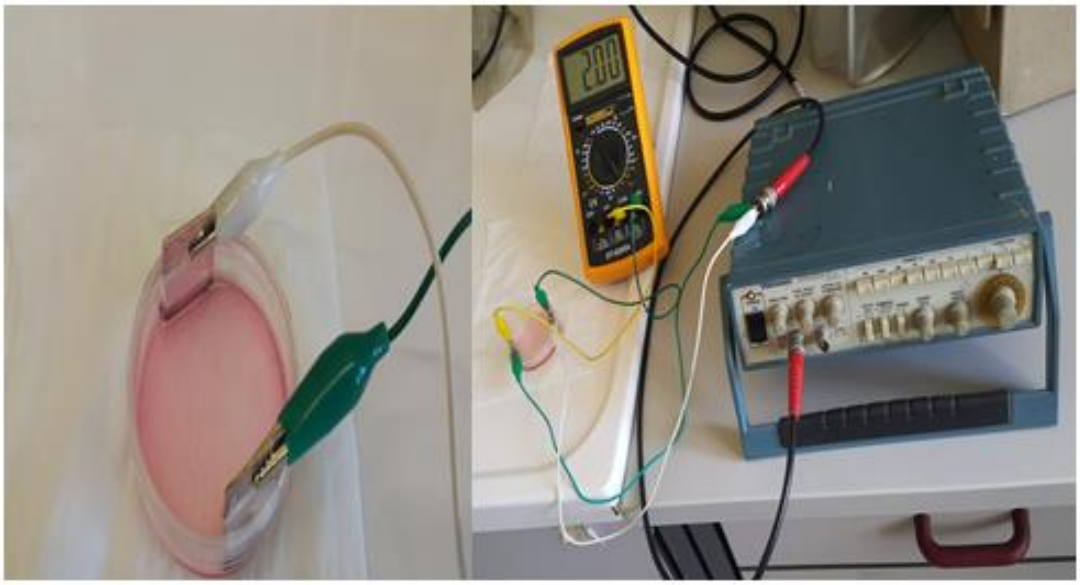

Figure 1. Electric field exposure system setup.

2.2. Cell culture

A human liver cancer cell line (HEPG2) was purchased from the National Institute of Oncology, Cairo, Egypt. The cells were cultured on collagen-coated tissue culture dishes (Sarstedt AG & Co, Nümbrecht, Germany) in a complete culture media of low glucose Dulbecco's Modified Eagle's Medium (DMEM) with L-Glutamine (Biowest, France), supplemented with 10% fetal bovine serum (FBS) (Biowest, France), 1% penicillin, and streptomycin (Biowest, France) and kept under standard cell culture conditions at 37 ℃ in a humidified CO_2 incubator containing 5% CO_2. Then, the medium was changed after 24 hours to remove the non-adherent cells. The cells were split every two or three days according to the degree of confluence (80−90%), and the cells were grown in a monolayer with a maximum passage number of 20.

2.3. The effect of different exposure frequencies on the examined cell line

The exposed groups (G1-G7) were subjected to different electric field frequencies (1 Hz, 10 Hz, 100 Hz, 1KHz, 10KHz, 100 KHz, 1 MHz) for 5 min, alongside the unexposed control group (Go). The following parameters were measured to determine the effect on each group: flow cytometry-apoptosis, fluorescent microscopy, gene expression analysis by polymerase chain reaction (PCR), and the dielectric properties.

2.3.1. Flow cytometry-apoptosis analysis

The viability was assessed using Annexin V and propidium Iodide (PI) staining solutions followed by a flow cytometry analysis that measured the number of cells. Annexin V and PI negative stains represented living cells [9].

The number of living/apoptotic/and necrotic cells was counted using a FACScan flow cytometer

(Becton Dickinson, San Diego, Calif, USA) in the CEERMA lab in the Faculty of Medicine, Alexandria University. The cells were exposed to an electric field and then incubated for 48 h. After incubation, the cells were subsequently washed with ice-cold PBS, trypsinized, and centrifuged at 2,000 g for 2 min. The cell pellet was resuspended in 1x binding buffer (10 mm HEPES/NaOH (pH 7.4), 140 mm NaCl, and 2.5 mm $CaCl_2$). Aliquots (100 µL) of the cell solution were mixed with 5 µL of Annexin V-FITC (BioVision, Milpitas, CA) and 10 µL of PI stock solutions (50 µg/mL in PBS) via gentle vertexing, followed by 15 min of incubation at room temperature in the dark. 400 µL of 1x binding buffer was added to each sample, followed by the flow cytometry analysis.

2.3.2. Fluorescent microscopy

The viability and permeability of the cell membranes and the nuclei of the living cells were evaluated by confocal microscopy. Hoechst 33342 (HOE) and PI are frequently used together for a simultaneous flow cytometric and fluorescence imaging analysis of the stages of apoptosis and cell-cycle distribution. Since Hoechst can readily cross cell membranes to stain the DNA of living and dead cells, it was used to label the total number of cells. In contrast, PI only enters cells with compromised plasma membranes, thus selectively labeling dead cells [10].

8 cell culture plates were prepared by inserting two coverslips in the base of each plate using sterilized forceps. The flask of culture cells was split and counted. $5 \cdot 10^4$ cells were seeded into each plate. Each coverslip was transferred to a well of six-well plates. The cells were fixed using 2 ml of 4% paraformaldehyde for 15 minutes at 37 °C, washed three times with 1X PBS, and stained with 1 ml of HOE (10 µg/mL) for 15 minutes in the dark at 37 °C. 1 ml of PI (10 µg/mL) was added to the wells, incubated in the dark for 15 minutes at 37°C, and washed again to remove the excess stain. Finally, the cells were observed under confocal microscopy (Leica) with excitations and emissions at 350 and 461 nm for HOE and at 493 and 636 nm for PI.

2.3.3. Gene expression analysis by polymerase chain reaction (PCR)

A PCR was applied to amplify the DNA fragments. The principle of PCR is that the associated primers with a DNA fragment can be extended by the DNA polymerase repeats of denaturing, annealing, and extension steps, thus allowing for the amplification of a DNA fragment from one copy to a billion copies [11]. A PCR reaction with primers for GADPH was performed for the internal control. A threshold was set to subtract the background. When the fluorescent intensity reached the threshold, the level of transcripts was recorded as the cycle threshold (C_T) [12], where

$$\Delta C_T \text{ (exposed group)} = C_T \text{ (exposed group target)} - C_T \text{ (exposed group reference (GADPH))} \quad (1)$$

$$\Delta C_T \text{ (control)} = C_T \text{ (control)} - C_T \text{ (control (GADPH))} \quad (2)$$

2.3.4. Dielectric properties measurement

The dielectric properties of cell line suspensions were determined using a commercial LCR meter (Fluke, Versatile, Automatic RCL Meters Technical Specifications PM 6306). The relative permeability and the conductivity were calculated by the mathematical relationships of capacitance and resistance in the frequency range of 50 Hz–1 MHz as follows:

$$\grave{\varepsilon} = \frac{capacitance\ of\ the\ cell\ suspension}{\text{Air capacitance}}, \quad (3)$$

$$\text{Air capacitance} = \frac{\epsilon o\ A}{d}\ , \quad (4)$$

$$\sigma = \frac{d}{R\ A}\ , \quad (5)$$

where ϵo is the permittivity of vacuum, which is equal to $8.85 \cdot 10^{-12}$ Farad/ meter, A is the surface area of the electrode, d is the distance between the two electrodes in meters, R is the resistance of the cell suspensions in ohms Ω, and σ is the conductivity in Simens/meter [13].

2.4. Statistical analysis

All data were expressed as mean ± standard deviation (SD) from three independent repeats. An analysis of variance (ANOVA) was used to evaluate the difference between multiple groups. Significant differences between the experimental groups were determined using a two-tailed Student's t-test (Excel 2013 Microsoft, USA). The results of the comparison between the cell viability of the studied groups according to flow cytometry results, the comparison between the studied groups according to HOCHEST 33342 and PI, and the comparison between the studied groups according to the cyclins (A, B, and E) activities were considered statistically significant when the p-value < 0.05.

3. Results

3.1. Flow cytometry viability analysis

Table 1 and Figure 2 display comparisons of all exposed groups to the control group. There was a significant decrease in the number of survived cells. Specifically, at frequencies 10^4 Hz and 10^5 Hz, there were mortality percentages of (57.11%) and (39.68%), respectively.

Table 1. Comparison between the cell viability of the studied groups according to flow cytometry results (mean ± SD).

	Control (n = 5)	G1 (n = 5)	G2 (n = 5)	G3 (n = 5)	G4 (n = 5)	G5 (n = 5)	G6 (n = 5)	G7 (n = 5)
Normal cells	90.93 ± 0.04	75.04 ± 0.08	71.19 ± 0.4	67.74 ± 0.36	73.44 ± 0.34	42.89 ± 0.06	60.32 ± 0.23	67.08 ± 0.33
Necrotic cells	3.17 ± 0.44	14.78 ± 0.04	7.07 ± 0.08	6.62 ± 0.09	8.31 ± 0.06	27.18 ± 0.12	15.37 ± 0.05	14.38 ± 0.02
Early apoptotic cells	4.71 ± 0.07	7.21 ± 0.06	18.6 ± 0.21	22.08 ± 0.05	13.32 ± 0.03	17.01 ± 0.06	17.80 ± 0.03	13.00 ± 0.07
Dead cells	1.19 ± 0.07	2.97 ± 0.04	3.14 ± 0.03	3.57 ± 0.06	4.92 ± 0.05	12.92 ± 0.03	6.51 ± 0.08	5.54 ± 0.09

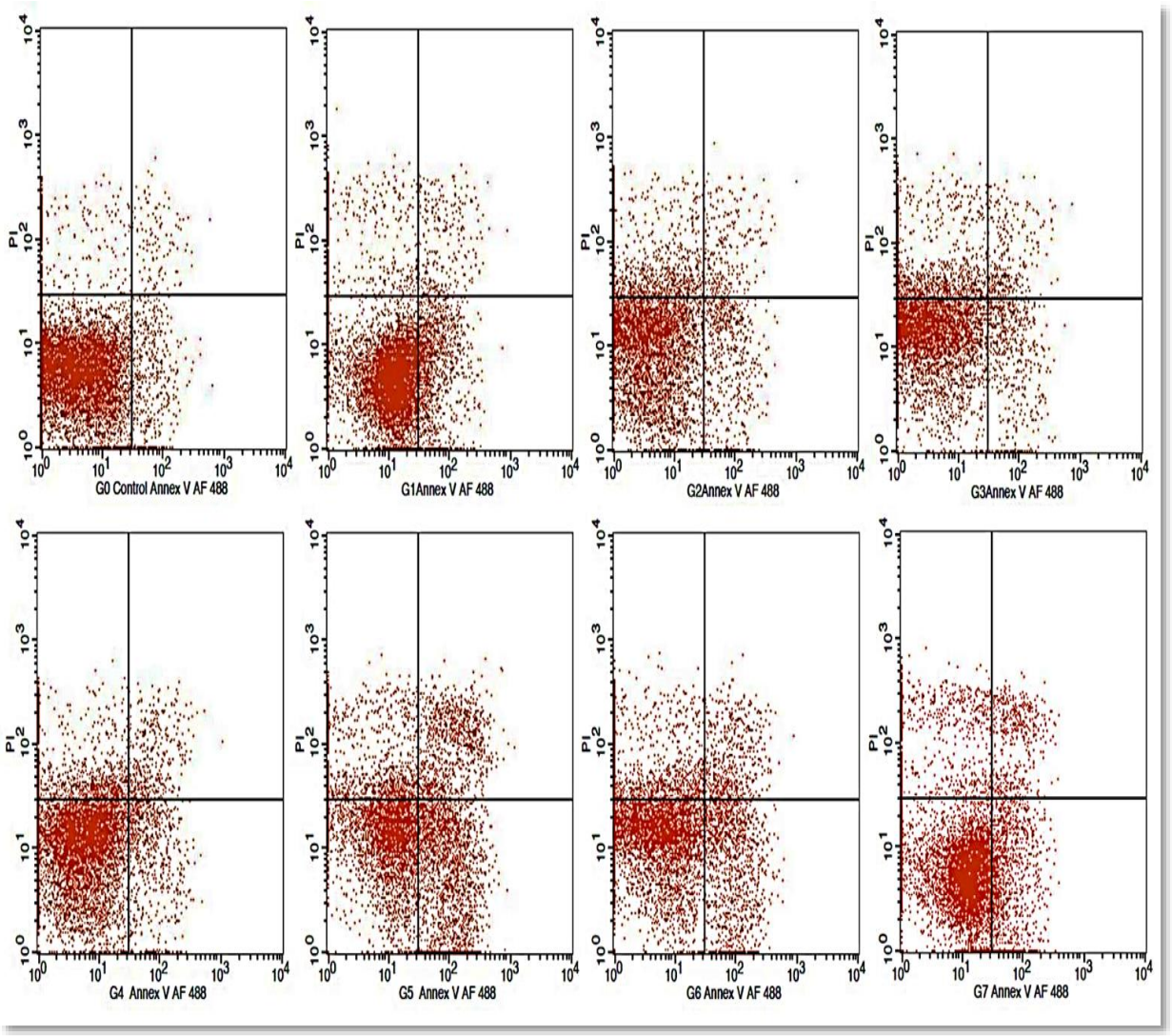

Figure 2. Flow cytometry images of exposed groups compared to the control group.

3.2. Viability and permeability detection using fluorescent microscopy

The permeability of each group was observed using a Leica fluorescence microscope and the fluorescent stains HOECHST 33342 (Figure 3) and PI (Figure 4), which are used for membrane integrity and nuclei staining. Using the Image J software, the fluorescence intensity was measured five times for each group. Compared to the control group, the HOECHST 33342 intensity was significantly lower in all exposed groups, while the PI intensity was significantly higher. In comparison to the control group, the three frequencies of 10^4 Hz, 10^5 Hz, and 10^6 Hz showed the highest significant rise in PI fluorescent intensity and the most significant reduction in HOECHST 33342 fluorescence intensity, thus indicating the influence of higher frequencies of AC electric fields, as shown in Table 2.

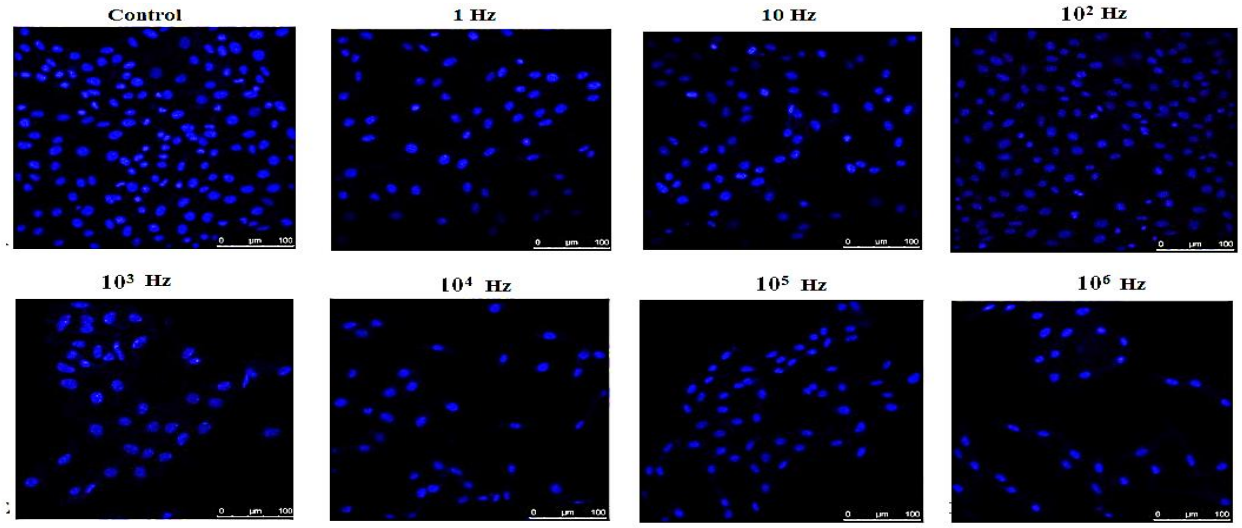

Figure 3. Cell viability detection using Hoechst33342 fluorescence staining of HepG2 exposed to different frequencies of electric fields after 48 hours of incubation.

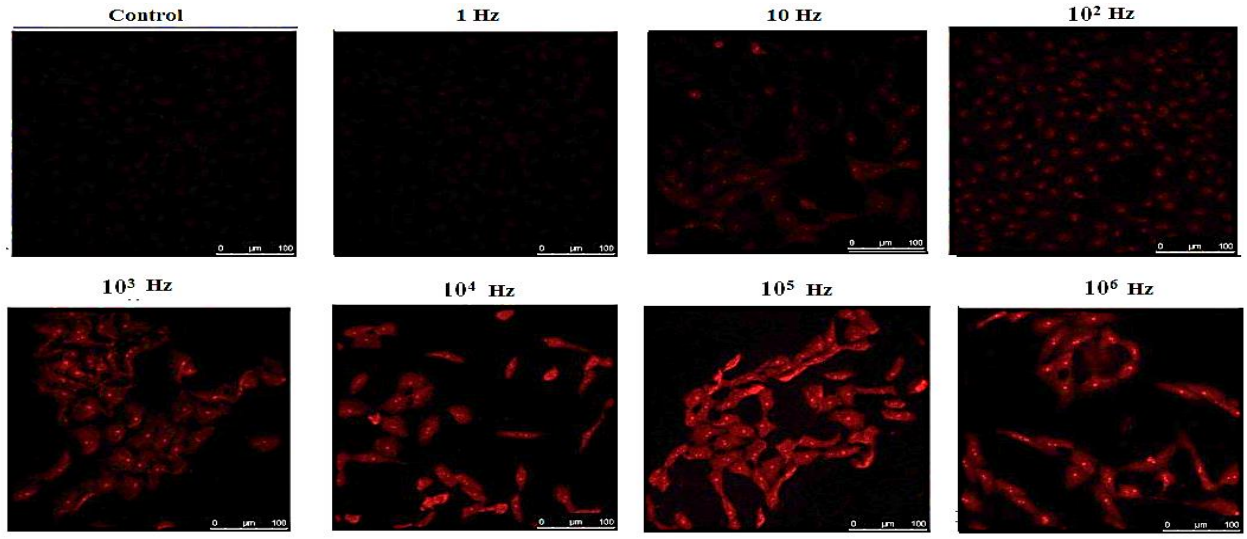

Figure 4. Apoptotic cell detection using propidium iodide fluorescence staining of HepG2 exposed to different frequencies of electric fields after 48 hours of incubation.

Table 2. Comparison between the studied groups according to HOCHEST 33342 and PI (mean ± SD).

	Control (n = 5)	G1 (n = 5)	G2 (n = 5)	G3 (n = 5)	G4 (n = 5)	G5 (n = 5)	G6 (n = 5)	G7 (n = 5)
HOCHEST 33342	28.3 ± 2.7	18.3 ± 2.3	19.1 ± 2.8	17 ± 0.8	15 ± 1.7	13.3 ± 0.6	12.8 ± 2.7	11.5 ± 2.6
PI	0.027 ± 0.038	0.034 ± 0.047	2.98 ± 1.59	2.55 ± 0.84	7.43 ± 1.08	14.2 ± 3.89	16.69 ± 1.68	9.99 ± 4.31

3.3. Gene expression analysis by PCR

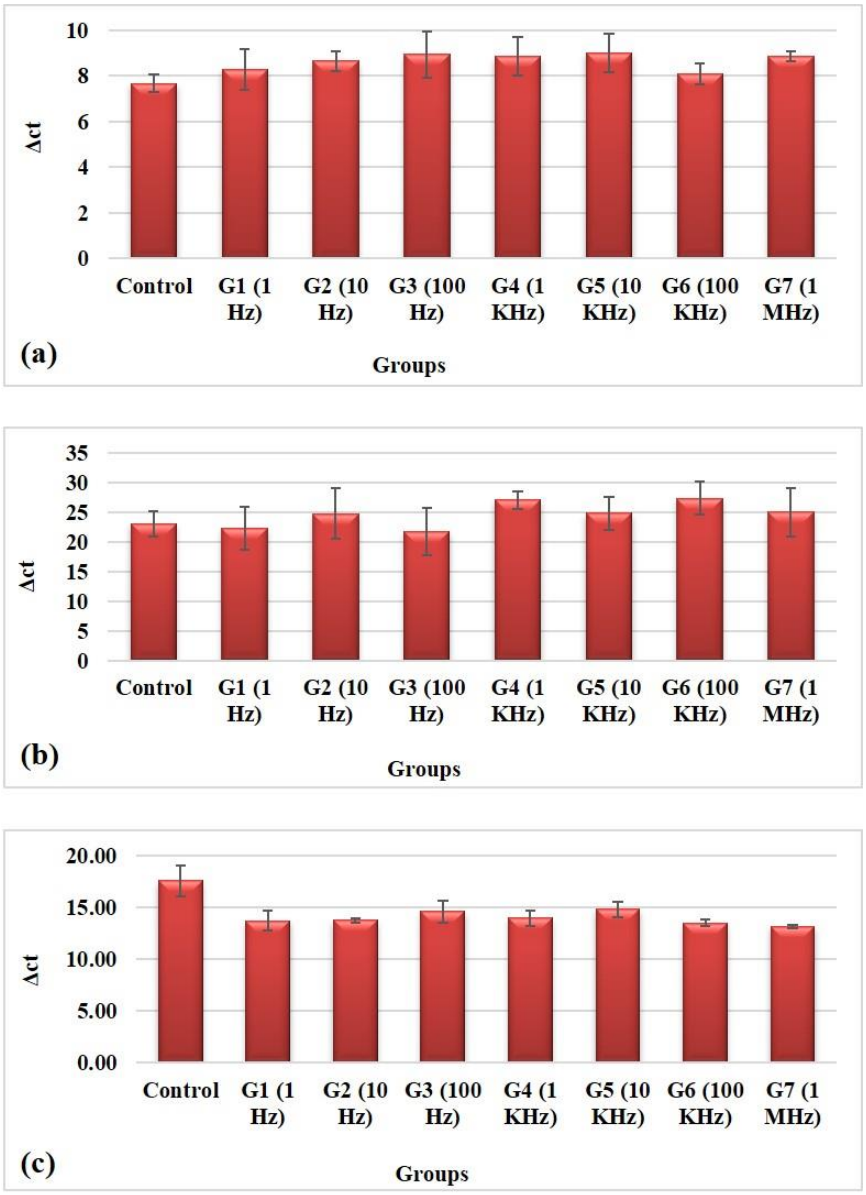

Figure 5. Cyclins activity for control and the groups exposed to different frequencies of electric fields; (a): Cyclin A, (b): Cyclin B, and (c): cyclin E.

The housekeeping gene GADPH and the cyclins A, B, and E were subjected to a quantitative real-time PCR to assess the genetic impact of exposure to various AC frequencies. Cyclins A and B showed no significant differences from the control group, as shown in Figures 5 a and b, respectively. Cyclin E, which is implicated in several biological processes related to hepatocarcinogenesis such as unchecked cell proliferation, invasion, and DNA damage, showed a substantial decrease in the exposed group (Figure 5c). A reduction in the tumor burden as it progresses can relate to the notable drop in cyclin E as compared to the control.

3.4. Dielectric properties determination

In the frequency range of 50 Hz to 1 MHz, the relative permittivity (έ) of the exposed groups compared to the control group was computed. The tissue's ability to store electric energy in the form of electric dipoles was measured by έ, as shown in Figure 6. The results show that while there was a noticeable rise in έ of the other exposed groups compared to control, there was almost no change between control and 1 Hz. The groups at 10 and 100 Hz were identical. While the έ values in the 1MHz group were close to 1 KHz, the difference became more noticeable starting at 1 KHz and reaching its maximum at 10 KHz and 100 KHz.

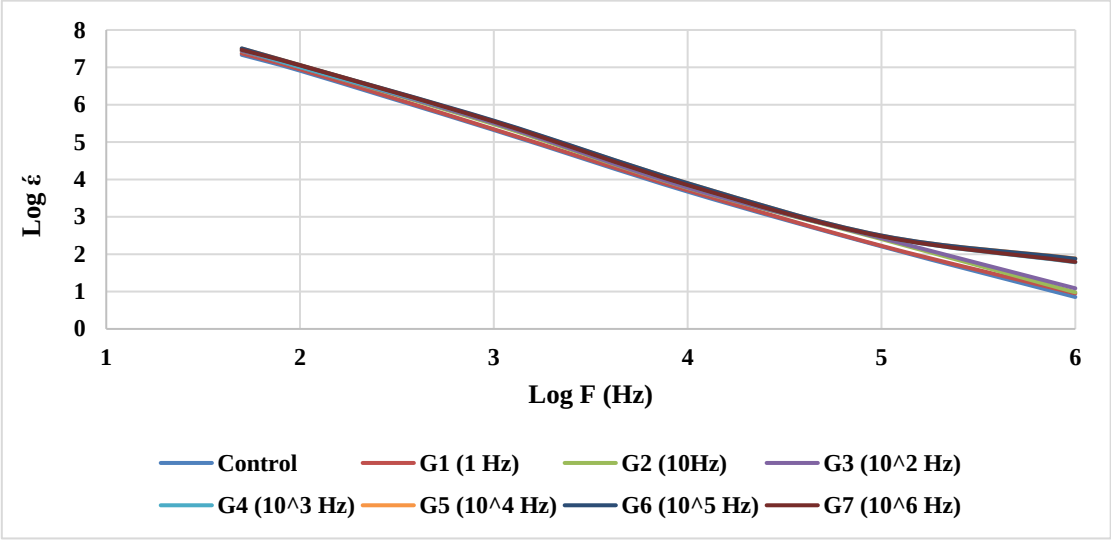

Figure 6. Log έ against Log frequency (Hz) in the frequency range from 50 Hz to 1 MHz for control and the exposed groups.

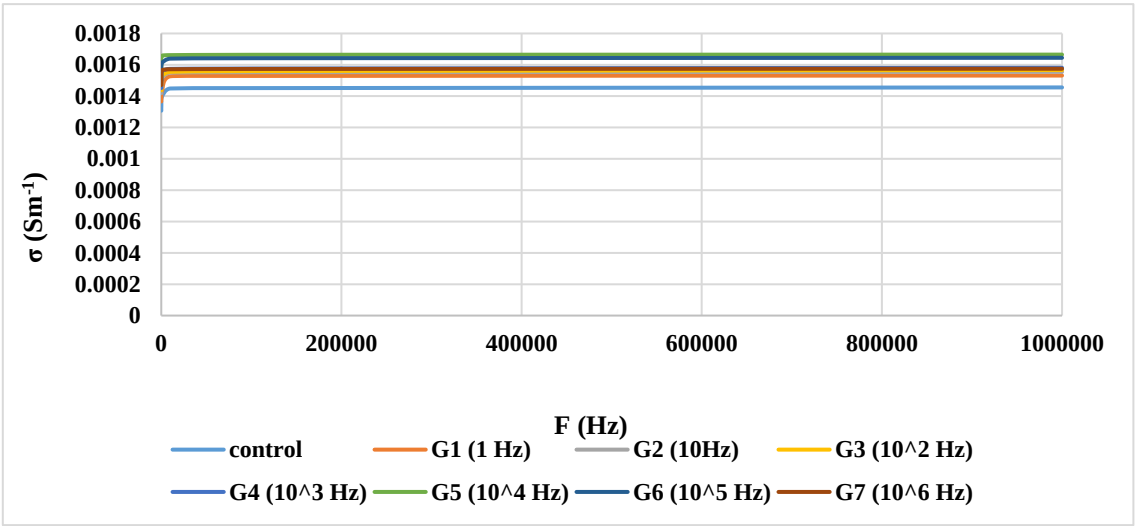

Figure 7. Electric conductivity (σ) in S m^{-1} against frequency (F) in Hz in the frequency range from 50 Hz to 1 MHz for control and the exposed groups.

The density and mobility of ions that move in the extracellular or intracellular regions by an applied electric field are measured by a tissue's electrical conductivity (σ). The difference between the exposed and control groups' σ was computed within the 50 Hz–1 MHz frequency range. According to our findings, σ gradually increased for each exposed group in the correct sequence, and each exposed group outperformed the control group. Groups 2, 3, and 4 had the lowest σ values, while Groups 5 and 6 had the highest values, as shown in Figure 7. The σ findings corroborate the ἐ data, which shows that the biggest influence occurs between 10 KHz and 100 KHz, whereas the major effect begins at the 1 KHz group.

4. Discussion

Trials for efficient alternatives to the current traditional cancer treatment methods have been attracting broad interest and attention. One of the most prominent factors for the application of the electric field is the frequency. Direct electric current (DC), which can be considered as a zero frequency, was used as an efficient disinfectant alternative, though it is not an optimum choice for cancer treatments due to electrolysis reactions and the massive production of free radicals [14].

Several reports documented the effect of different AC conditions on the viability and/or permeability of different types of cancer cells. Different electrical conditions can lead to various biological mechanisms such as electrochemotherapy [15], electroendocytosis [16], irreversible electroporation [17], and tumor-treating fields [18].

In the current work, we aimed to only change the frequency in a wide range (1 Hz−1 MHz) and to set all the other electrical conditions to be constant without targeting a certain mechanism to detect the biological response solely to the electric frequency parameter.

Our findings demonstrated that the highest anti-tumoral effect on HEPG2 was found at 10 KHz followed by the impact of 100 KHz with 57.11% and 39.68% of the cells undergoing stages of death, respectively. These results culminated in a defined mortality rate that was identified by flow cytometry analysis. The impact of 100 KHz can be correlated to the tumor-treating fields (TTFs) effect which blocks cell proliferation, thus leading to growth inhibition through the selective disruption of the ability of the cancer cells to divide by inhibiting mitotic spindle formation during metaphase by the application of a low electric field at 100−300 KHz [19]. However, the anti-tumoral effect of 10 KHz, which was significantly higher than the impact of 100 KHz, can be postulated as either the effect of efficiently starting the TTFs technique at 10 KHz, and not at 100 KHz as thought in previous reports; alternatively, there is a specific biophysical phenomenon which begins at 10 KHz that has not been specified yet, which should attract some level of interest.

The flow cytometry results were confirmed by PI and HOECHST 33342 results. PI was employed as a fluorescent marker in which a tiny and rapid absorption of PI, which penetrates through the pores and specifically binds to DNA and RNA, may come from the electro-permeabilization of the plasma membrane, as represented by an increase of red fluorescent areas through the uptake of PI into cells [20]. HOECHST 33342 staining of HepG2 culture cells highlighted the nucleus in blue and enabled the observation and characterization of the culture's shape, growth state, and survival [21]. The HOECHST 33342 fluorescence intensity significantly decreased at frequencies of 10 KHz and 100 KHz, thus confirming the rate of cell death. The fluorescence investigations reflected the chemical changes caused by the applied frequencies. Considerable increases in the cell permeability were corroborated by the detection of a considerable rise in the PI fluorescence intensity at frequencies of

10 KHz and 100 KHz.

Chromosomal segregation, cell division, and DNA replication are all parts of the eukaryotic cell cycle. Complexes that consist of cyclins bound to cyclin-dependent protein kinases (CDKs) control the mitotic cycle [22]. In several tumor types, including HCC, the upregulation of cyclin family proteins is typically associated with advanced stages and unfavorable outcomes. Independent of its conventional interaction partner, CDK2, cyclin E, a regulator of the cell cycle, is a key modulator and biomarker of the progression of liver cancer in mice and humans. The overexpression of cyclin E during diagnosis is associated with several biological processes, such as invasion, stemness, DNA damage response, proliferation, and the tumor microenvironment; Cyclin E1 stimulates CDK2 and starts DNA replication to promote cell division [23]. Our findings indicated a considerable decrease in cyclin E but no significant change in cyclins A or B. Cyclin E reduction during intervention significantly reduces the tumor burden as liver cancer advances [24]. A further study is required to correlate the effect of 10 KHz on cyclin E to detect its mechanism of action.

The results of this investigation demonstrated that, while the exposed groups' relative electric permittivity and conductivity noticeably increased compared to the control, there was no change between the control and 1 Hz groups. Between the groups, there was no difference at 10 and 100 Hz. The significant increase became more noticeable at 1 KHz. The values in the 1MHz group were comparable to 1 KHz, while the difference was the largest between 10 KHz and 100 KHz. With the relation of the control group, the exposed groups' relative permittivity and conductivity increased, thus reflecting the various current pathways and dispersions within and outside the cells based on the exposure frequency.

5. Conclusions

According to the present study, we conclude the following:

- The anti-tumor frequency effect of the AC electric field became more present on the HEPG2 from 1 KHz to 1 MHz.
- The most effect on the viability of cells was noticed at the two frequencies of 10 KHz with a death ratio of (57.11%) and 100 KHz with a death ratio of (39.68%).
- The greatest significant reduction of HOECHST 33342 fluorescent intensity and the greatest increase in PI fluorescent intensity was found at the three frequencies of 10KHz–1 MHz compared to the control group, which assures the effect of the higher frequencies of AC electric fields.
- The significant reduction in cyclin E compared with control can be correlated with the reduction of the tumor burden during its progression.
- The dielectric permittivity and conductivity both increased alongside the control group, which indicates the change in the cell dielectric properties after exposure to the AC electric fields.

Use of generative-AI tools declaration

The authors declare they have not used artificial intelligence (AI) tools in the creation of this article.

Conflict of interest

All authors declare no conflicts of interest in this paper.

Author contributions

Moataz M. Fahmy, Sohier M. El-Kholey, Seham Elabd, and Mamdouh M. Shawki conceived the idea, put the general design of the research, collected literature data, preparing tables and figures, writing the first draft and reviewing the final manuscript. Mamdouh M. Shawki and Moataz M. Fahmy performed experiment related to electricity. Seham Elabd performed cellular experiments. Mamdouh M. Shawki and Sohier M. El-Kholey general administration and contributed to the reviewing process.

References

1. Llovet JM, Kelley RK, Villanueva A, et al. (2021) Hepatocellular carcinoma. *Nat Rev Dis Primers* 7: 6. https://doi.org/10.1038/s41572-020-00240-3
2. Bray F, Ferlay J, Soerjomataram I, et al. (2018) Global cancer statistics 2018: GLOBOCAN estimates of incidence and mortality worldwide for 36 cancers in 185 countries. *CA Cancer J Clin* 68: 394−424. https://doi.org/10.3322/caac.21492
3. Marrero JA, Laura MK, Claude BS, et al. (2018) Diagnosis, staging, and management of hepatocellular carcinoma: 2018 practice guidance by the American Association for the Study of Liver Diseases. *Hepatology* 68: 723–750. https://doi.org/10.1002/hep.29913
4. Villemejane J, Mir LM (2009) Physical methods of nucleic acid transfer: general concepts and applications. *Br J Pharmacol* 157: 207–219. https://doi.org/10.1111/j.1476-5381.2009.00032.x
5. Kirson ED, Gurvich Z, Schneiderman R., et al. (2004) Disruption of cancer cell replication by alternating electric fields. *Cancer Res* 64: 3288–3295. https://doi.org/10.1158/0008-5472.CAN-04-0083
6. Zhang Y, Liang H, Tan H, et al. (2020) Development of microfluidic platform to high-throughput quantify single-cell intrinsic bioelectrical markers of tumor cell lines, subtypes and patient tumor cells. *Sensor Actuat B-Chem* 317: 128231. https://doi.org/10.1016/j.snb.2020.128231
7. Cone D (1971) Unified theory on the basic mechanism of normal mitotic control and oncogenesis. *J Theor Biol* 30: 151–181. https://doi.org/10.1016/0022-5193(71)90042-7
8. Al Ahmad M, Al Natour Z, Mustafa F, et al. (2018) Electrical characterization of normal and cancer cells. *IEEE Access* 6: 25979−25986. https://doi.org/10.1109/ACCESS.2018.2830883
9. Manatunga DC, De Silva RM, Nalin KM, et al. (2018) Effective delivery of hydrophobic drugs to breast (MCF-7) and Liver (HepG2) cancer cells: a detailed investigation using cytotoxicity assays, fluorescence imaging and flow cytometry. *Eur J Pharm Biopharm* 128: 18−26. https://doi.org/10.1016/j.ejpb.2018.04.001
10. Tummala V, Jaiswal J, Singh AK, et al. (2022) Biosynthesized silver nanoparticles having high redox current enhance anticancer response for HepG2 cells. *Iran J Sci Technol Trans Sci* 46: 1531–1539. https://doi.org/10.1007/s40995-022-01374-7
11. Kadri K (2019) Polymerase chain reaction (PCR): principle and applications in: perspectives on polymerase chain reaction, *Synthetic Biology, New Interdisciplinary Science*. https://doi.org/10.5772/intechopen.86491

12. Bustin SA, Benes V, Nolan T, et al. (2005) Quantitative real-time RT-PCR—a perspective, *J Mol Endocrinol*. 34: 597–601. https://doi.org/10.1677/jme.1.01755
13. Ambujakshi NP, Raveesha HR, Manohara SR, et al. (2019) Chonemorpha grandiflora extract mediated synthesis of Ag-ZnO nanoparticles for its anticancer, electrical and dielectric applications. *Mater Res Express* 6: 095068. https://doi.org/10.1088/2053-1591/ab3022
14. Camué Ciria HM, González MM, Zamora Lo, et al. (2013) Antitumor effects of electrochemical treatment. *Chin J Cancer Res* 25: 223–234. dohttps://10.3978/j.issn.1000-9604.2013.03.03
15. Morozas A, Malyško-Ptašinskė V, Kulbacka J, et al. (2024) Electrochemotherapy for head and neck cancers: possibilities and limitations. *Front Oncol* 14: 1353800. https://doi.org/10.3389/fonc.2024.1353800
16. Abd-Elghany AA (2022) Incorporation of electroendocytosis and nanosecond pulsed electric field in electrochemotherapy of breast cancer cells. *Electromagn Biol Med* 41: 25−34. https://doi.org/10.1080/15368378.2021.1978479
17. Prabhakar P, Avudaiappan AP, Sandman M, et al. (2024) Irreversible electroporation as a focal therapy for localized prostate cancer: a systematic review. *Indian J Urol* 40: 6−16. https://doi.org/10.4103/iju.iju_370_23
18. Mun EJ, Babiker HM, Weinberg U, et al. (2018) Tumor-treating fields: a fourth modality in cancer treatment. *Clin Cancer Res* 24: 266−275. https://doi.org/10.1158/1078-0432.CCR-17-1117
19. Giladi M, Weinberg U, Schneiderman RS, et al. (2014) Alternating electric fields (tumor-treating fields therapy) can improve chemotherapy treatment efficacy in non-small cell lung cancer both in vitro and in vivo. *Semin Oncol* 41: S35–S41. https://doi.org/10.1053/j.seminoncol.2014.09.006
20. Xiao D, Yao C, Liu H, et al. (2013) Irreversible electroporation and apoptosis in human liver cancer cells induced by nanosecond electric pulses. *Bioelectromagnetics* 34: 512−520. https://doi.org/10.1002/bem.21796
21. Jing BW, Wen Q, Zhuo Y, et al. (2022) Optimization of three-dimensional culture conditions of HepG2 cells with response surface methodology based on the VitroGel system. *Biomed Env Sci* 35: 688−698. https://doi.org/10.3967/bes2022.091
22. El-Aouar RA, Nicolas A, De Paula TL, et al. (2017) Heterogeneous family of cyclomodulins: smart weapons that allow bacteria to hijack the eukaryotic cell cycle and promote infections. *Front Cell Infect Microbiol* 7: 208. https://doi.org/10.3389/fcimb.2017.00208
23. Xu J, Huang F, Yao Z, et al. (2019) Inhibition of cyclin E1 sensitizes hepatocellular carcinoma cells to regorafenib by mcl-1 suppression. *Cell Commun Signal* 17: 85. https://doi.org/10.1186/s12964-019-0398-3
24. Sonntag R, Penners C, Kohlhepp M, et al. (2021) Cyclin E1 in murine and human liver cancer: a promising target for therapeutic intervention during tumour progression. *Cancers (Basel)*13: 5680. https://doi.org/10.3390/cancers13225680

AIMS Press